Robustness and uncertainty of projected changes in the impacts of Typhoon Vera (1959) under global warming

Tetsuya Takemi[1], Rui Ito[2] and Osamu Arakawa[3]

[1]Disaster Prevention Research Institute, Kyoto University, Japan
[2]National Research Institute for Earth Science and Disaster Resilience, Japan
[3]Faculty of Life and Environmental Sciences, University of Tsukuba, Japan

Abstract:

This study numerically investigates the influences of global warming on Typhoon Vera (1959) by conducting pseudo-global warming experiments. It was found that the intensity of Typhoon Vera will be stronger in warmed climate conditions than in the actual September 1959 condition not only at the time of the typhoon's maturity but also at the time of the landfall. Sensitivity experiments indicate that this projected increase in the typhoon intensity is robust, by taking into consideration the effects of the increase in sea surface temperature and temperature lapse rate under global warming. The examination of rainfall characteristics over the Kiso River and the Yodo River basin demonstrated that the maximum accumulated rainfall and the maximum hourly rainfall at a certain location within the region are more intensified in the PGW conditions than in the 1959 condition at their worst levels. Robustness and uncertainty of the projected changes in the typhoon impacts are discussed.

KEYWORDS typhoon; global warming; impact assessment; pseudo-global warming experiment

INTRODUCTION

Typhoon Vera (1959), known as Isewan Typhoon, is the worst case among the disaster-spawning extreme weather in terms of human losses at least over the past 100 years (National Astronomical Observatory of Japan, 2015). There were more than 5000 fatalities and missing, and about 39000 injured. The typhoon caused strong wind, storm surge, and heavy rainfall, inducing devastating damages in Japan. According to the best-track data of Japan Meteorological Agency (JMA), the minimum central surface pressures during the lifetime and the central surface pressure at the time of landfall were 895 hPa and 929 hPa, respectively. Isewan Typhoon, Muroto Typhoon (1934), and Makurazaki Typhoon (1945) are commonly known as the three major typhoons in Showa Period (i.e., 1926–1989) in Japan. Global warming is considered to strengthen the intensity of such extreme tropical cyclones (TCs) (e.g., Murakami *et al.*, 2012), and therefore, assessing the influences of global warming on extreme TCs is an important issue in order to respond to and mitigate disaster risks in a future climate.

Assessing the impacts of extreme weather requires high-resolution numerical simulations, because a precise representation of topography is important (Oku *et al.*, 2010).

Thus, conducting dynamical-downscaling numerical experiments is a prerequisite for impact assessment applications. To conduct downscaling experiments for past events, a long-term reanalysis dataset is useful. The Japanese 55-year Reanalysis (JRA-55), available after 1958 (Ebita *et al.*, 2011; Kobayashi *et al.*, 2015; Harada *et al.*, 2016), is useful in reproducing historical events in numerical simulations. We take advantage of this reanalysis dataset.

The influences of future global warming on a specific event are examined with the use of a pseudo-global warming (PGW) experiment approach (Sato *et al.*, 2007). The PGW experiment approach is a powerful tool to quantify the climate change influences on a specific event by separating the increments of climate change from the past meteorological fields (Takemi *et al.*, 2016b), and has been applied for investigating the influences of global warming on Typhoon Songda (2004) (Ito *et al.*, 2016) and on Typhoon Mireille (1991) (Takemi *et al.*, 2016a). A similar idea to the PGW approach was employed to investigate the climate change effects on the worst storm surge generated by Typhoon Haiyan (2013) (Takayabu *et al.*, 2015).

In this study, we investigate the influences of global warming on the severity of Typhoon Vera (1959) by conducting downscaling experiments with a regional meteorological model. We focus on the projected changes in the intensity of Typhoon Vera simulated in the PGW experiments and changes in regional-scale rainfall characteristics by this typhoon. In Mori and Takemi (2016), preliminary analysis on the influences of global warming on Typhoon Vera was performed; this study extends their preliminary analysis to investigate global warming influences on Typhoon Vera by conducting a number of sensitivity experiments. Robustness and uncertainty of the projected changes in the intensity and rainfall characteristics of Typhoon Vera under warmed climate conditions are discussed.

NUMERICAL MODEL AND EXPERIMENTAL DESIGN

The numerical model used was the Weather Research and Forecasting (WRF) model/the Advanced Research WRF (ARW) version 3.3.1 (Skamarock *et al.*, 2008). Two-way nesting capability was employed to cover a wide region in the western North Pacific and to better represent the rainfall amount at a high-resolution. Figure 1 shows the computa-
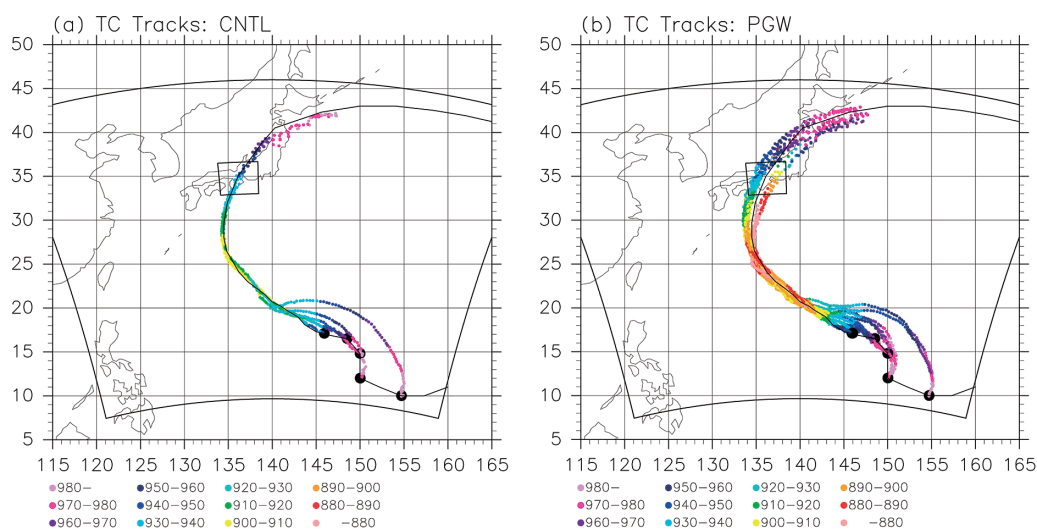
Figure 1. The computational domains (shown by solid lines): the outer area indicates Domain 1 and the inner area indicates Domain 2. The best track and the simulated tracks of the tropical cyclones (TCs) are indicated by black solid line and colored points, respectively, for (a) the September 1959 condition (CNTL) and (b) the PGW conditions. Each colored point denotes the central pressure (in hPa) of the TCs, and the color legend is given below each panel. See details in the main text for the CNTL and PGW conditions

tional domains. The outer domain (Domain 1) was defined in the Lambert conformal projection on the plane crossing the latitudes of 30°N and 60°N and centered at the point of 140°E and 27°N, with the grid numbers of 976 in the longitudinal direction and 831 in the latitudinal direction at the 5-km grid spacing. The nested domain (Domain 2) covered the Nobi Plain and its surrounding mountains and the Kinki district with the grid numbers of 401 by 401 at the 1-km grid spacing. Both domains had 56 vertical levels, with the interval being stretched with height and the top being the 20-hPa level.

Physics parameterizations were chosen in the same way as in Mori and Takemi (2016). For example, we chose the Yonsei University single-moment 6-class scheme for cloud microphysics (Hong and Lim, 2006), the Kain-Fritsch scheme for cumulus convection (applied only for Domain 1) (Kain, 2004), and the Yonsei University scheme for boundary-layer turbulent mixing (Hong *et al.*, 2006).

The initial and boundary conditions were given from the 6-hourly, 1.25°-resolution JRA-55 dataset for September 1959. The spectral nudging technique for low wave number components of middle- and upper-level winds was applied to keep the synoptic-scale influences on the simulated typhoons. To facilitate the intensification of typhoons, we inserted a TC-like vortex with the TC bogus scheme (Wang *et al.*, 2010) of the WRF model at positions according to the best-track data. See Supplement Text S1 for the discussion on the use of the TC bogus scheme in the present simulations. Kanada *et al.* (2016) also discuss the use of the TC bogus scheme in simulating typhoons.

In simulating Typhoon Vera under the September 1959 condition, sensitivity to the initial time for time integration was examined by changing the initial time from 1200 UTC 20 September to 1200 UTC 22 September 1959 with 12 hours interval. The group of 5 historical runs initialized at the different times are referred to as CNTL.

To conduct PGW experiments, incremental meteorologi-

cal variables from the present to the future climate are required. For this purpose, we used the climate simulation data from a 20-km-mesh atmospheric general circulation model (AGCM), i.e., MRI-AGCM Version 3.2 (Mizuta *et al.*, 2012) for the present climate and for the future climates under the Representative Concentration Pathway (RCP)-8.5 scenario (Kitoh and Endo, 2016; Kusunoki, 2016). The future climate states were driven with the ensemble mean sea surface temperature (SST) averaged for the Coupled Model Intercomparison Project Phase 5 (CMIP5) atmosphere-ocean coupled models and the three SST patterns derived from the cluster analysis on the CMIP5 models (Mizuta *et al.*, 2014). The PGW experiments with the increments from the AGCM run with the ensemble-mean SST are referred to as PGW0, while those with clustered SST patterns, i.e., Cluster 1, 2, and 3 in Mizuta *et al.* (2014), are referred to as PGW1, PGW2, and PGW3, respectively. The warming increment was defined as the difference in the monthly mean of September between the present and the future climate conditions. The warming increments of SST and surface air temperature are found in Supplement Figures S1 and S2, respectively. It is seen that the SST increments are 2–4 K, depending on the latitude. The warming increments were added to the JRA-55 field.

As in Ito *et al.* (2016), we did not add relative humidity and winds as warming increment, because of no significant difference in relative humidity from the present to the future (Takemi *et al.*, 2012) and of unwanted influences of wind fields on dispersing typhoon tracks. By excluding these variables from adding to JRA-55 as the warming increments, we examined in the PGW0 runs some combinations of meteorological variables that were added as the warming increments. The first case was to add SST, surface air temperature, surface pressure, and three-dimensional temperature and geopotential height as the increments (referred to as PGW0(SST/T/GHT)), the second was to add SST, surface air temperature, and three-dimensional temperature as the

increments (PGW0(SST/T)), and the third was to add only the SST increment (PGW0(SST)). The difference between the cases of PGW0(SST/T/GHT) and (PGW0(SST/T) is intended to examine the effects of temperature lapse rate on the intensity of the typhoons through separating the influences of geopotential height. The case of PGW0(SST) is an extreme case to examine how SST warming without the changes in the atmospheric stability affects the typhoon intensity. Note that in PGW1, PGW2, and PGW3 the list of added variables as the increments was the same as in PGW0(SST/T/GHT).

All the PGW0 cases are initialized at the 5 different times similar to the CNTL runs, while the runs of PGW1, PGW2, and PGW3 are initialized at 0000 UTC and 1200 UTC on 22 September. Each run name refers to the group of runs with different initial times.

RESULTS

Figure 1 compares the track and intensity of the simulated typhoons in the CNTL and the PGW conditions. The best track of Typhoon Vera (1959) is also indicated. In the CNTL cases, the simulated typhoons closely move along the best track after they pass the 20°N latitude (Figure 1a). The minimum central surface pressure during the simulated period ranges between 899.5 and 909.0 hPa, which agree well with the observed value of 895 hPa. In addition, the central pressure at the time of landfall (which was defined as the time when the simulated typhoon crosses the 33°N latitude), varying between 926.2 and 932.7 hPa, also agrees well with the observed value of 929 hPa. Because typhoon-induced rainfall and winds in a specific area sharply depend on the track and intensity of typhoons, the favorable agreement of the simulated typhoons in CNTL with the observation is important for assessing the meteorological hazards of typhoons.

In Figure 1b, the tracks in all the PGW experiments are plotted. It is seen that the simulated typhoons over the ocean become stronger in the PGW conditions than in CNTL. The tracks of the typhoons in the PGW conditions are slightly

dispersed from the best-track. Although slight changes in the typhoon tracks may not be of primary importance in investigating future changes in the intensity and structure of typhoons themselves, such track changes will significantly affect the assessment of the typhoon impacts on local-scale hazards (Mori *et al.*, 2014). We will examine later how the characteristics of rainfall appear in the PGW experiment in comparison to those in CNTL.

The maximum intensity of the typhoons during their lifetimes in the CNTL and the PGW conditions is exhibited in Figure 2 in terms of the minimum central surface pressure and the maximum surface wind speed around the TC center. Overall, the minimum central pressure is lower and the maximum wind speed is higher in PGW than in CNTL, irrespective of the initial times of the simulations, the added variables as the warming increments, and the AGCM future runs with different SST conditions. With SST and three-dimensional atmospheric fields considered as warming increments, the minimum central pressure and the maximum wind speed range between 879.4 and 898.1 hPa and 64.6 and 66.5 m s^{-1}, respectively. Under the extreme conditions in which only SST is added as warming increment, i.e., the PGW0(SST) cases, the minimum central pressure and the maximum wind speed are 859.7–876.8 hPa and 71.1–73.3 m s^{-1}. It is known that under future global warming the magnitude of temperature increase is larger in the upper troposphere than in the lower troposphere (Santer *et al.*, 2008; Thorne *et al.*, 2010; Takemi *et al.*, 2012), which indicates that the troposphere is stabilized from the viewpoint of temperature lapse rate. Therefore, in the PGW0(SST) cases, stabilizing effects on convective circulation in typhoons diminish and only the positive effects of the SST increase make the simulated typhoons extremely strong.

Figure 3 further compares the intensity of the simulated typhoons in the CNTL and the PGW conditions at the times of landfall (defined similarly as described previously). It is seen that in general the simulated typhoons are still stronger in PGW than in CNTL, except in some cases. The ranges of the central pressure and the maximum wind speed in the PGW conditions except for PGW0(SST) are 912.7–929.5 hPa and 49.8–55.1 m s^{-1}, respectively, while those for
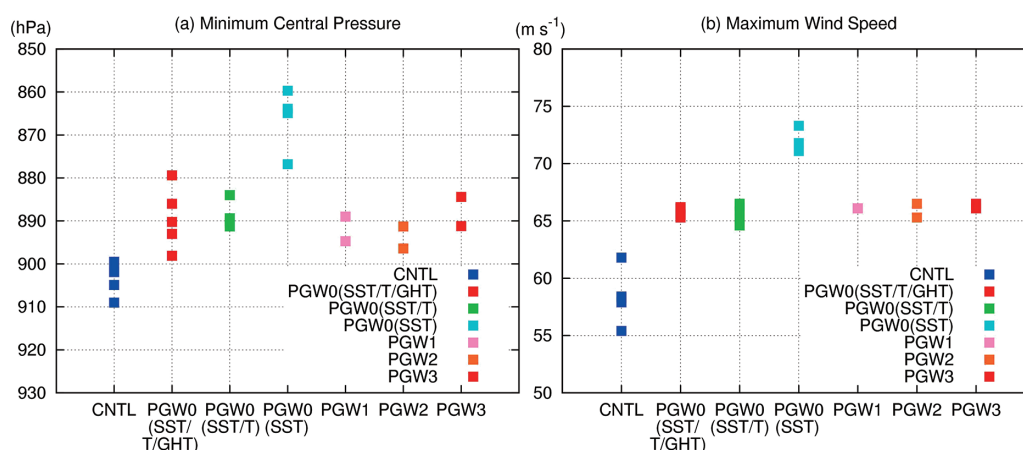

Figure 2. The intensity of the simulated typhoons at their maximum intensity in the CNTL and the PGW experiments: (a) minimum central surface pressure and (b) maximum surface wind speed. See the main text for the code names of the experiments
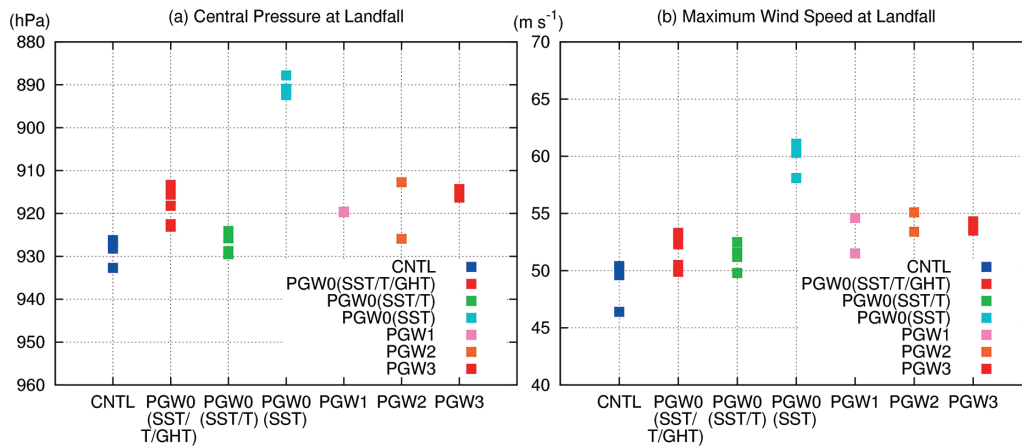
Figure 3. The same as Figure 2, except for the intensity of the simulated typhoons at the times of the landfall (when the typhoons cross the 33°N line)

the PGW0(SST) case are 887.8–892.4 hPa and 58.1–61.1 m s^{-1}. Therefore, the intensified strength of the simulated typhoons in warmed climate conditions is still maintained until they make landfall on the Pacific side of the Kinki and Chubu districts.

This projected change in the typhoon intensity has a clear contrast to the change in the intensity of Typhoon Songda (2004) at higher latitudes in PGW conditions. Note that because both Typhoon Vera (1959) and Typhoon Songda occurred in September the warming increments added to the JRA-55 fields for the two typhoons are exactly the same for both. Although the intensity of Typhoon Songda at its maximum is stronger in PGW conditions than in the actual September 2004 condition, the simulated typhoons in PGW conditions rapidly weaken as they move northward; the intensity of the typhoons when they are located around Hokkaido is weaker in PGW than in the actual condition (Ito *et al.*, 2016). Different from the rapid weakening of Typhoon Songda in the northern part of Japan in PGW conditions, the intensified strength of Typhoon Vera in the PGW conditions is maintained until it makes landfall. We then examine how the intensified typhoons in the PGW conditions affect regional-scale rainfall characteristics.

Because Typhoon Vera (1959) caused heavy rainfall over the Kiso River and the Yodo River basin (JMA, 1961) and significant amounts of river discharge occurred over these basins, the analysis on the rainfall characteristics is focused on those regions. Figure 4 displays the areas in the Chubu and Kinki districts for analyzing the rainfall within the Kiso River and the Yodo River basin, respectively. The positions of the simulated typhoons as well as the best-track of Typhoon Vera (1959) are also plotted in Figure 4. We examined the area-mean total rainfall averaged over each analysis area, the area-maximum total rainfall at any grid within each analysis area, and the area-maximum hourly rainfall at any grid within each area. The hourly outputs from Domain 2 during the period from 0000 UTC 23 September to 1200 UTC 27 September were used for this analysis. The total rainfall refers to the accumulated amount during this period.

Figure 5 indicates these rainfall characteristics in the area of the Chubu district against the longitudinal positions at the landfall times. Except for the PGW0(SST) cases, the CNTL
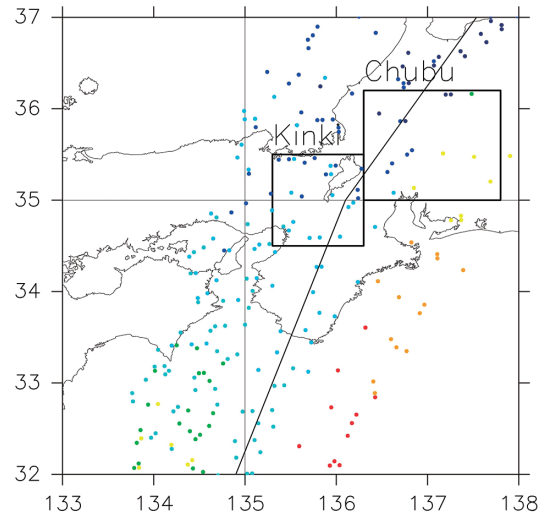

Figure 4. The Chubu and Kinki areas (indicated by boxes) to assess the rainfall amount in the CNTL and the PGW experiments. The positions of the typhoon centers are also indicated by colored marks (the color legend is the same as in Figure 1)

cases reproduces larger amounts of area-mean total rainfall than the other PGW cases (Figure 5a). The area-mean total rainfall seems to depend on the location of the typhoon landfall. Only a case among the PGW0(SST) experiments shows a larger amount of the mean total rainfall than the CNTL cases. Although the intensity of the simulated typhoons in the PGW conditions is mostly stronger than that in the CNTL cases at the times of landfall as well as the typhoons' maturity, the mean total rainfall seems to be more controlled by the landfall location.

As far as the area-maximum total rainfall in the Chubu area is concerned, the features appear differently. Figure 5b shows that there are a number of the PGW cases in which more maximum total rainfall occurred at a certain grid in the Chubu area compared with the CNTL cases. One case in PGW0(SST) indicates an extreme rainfall exceeding 500 mm, which is remarkably larger than the values in
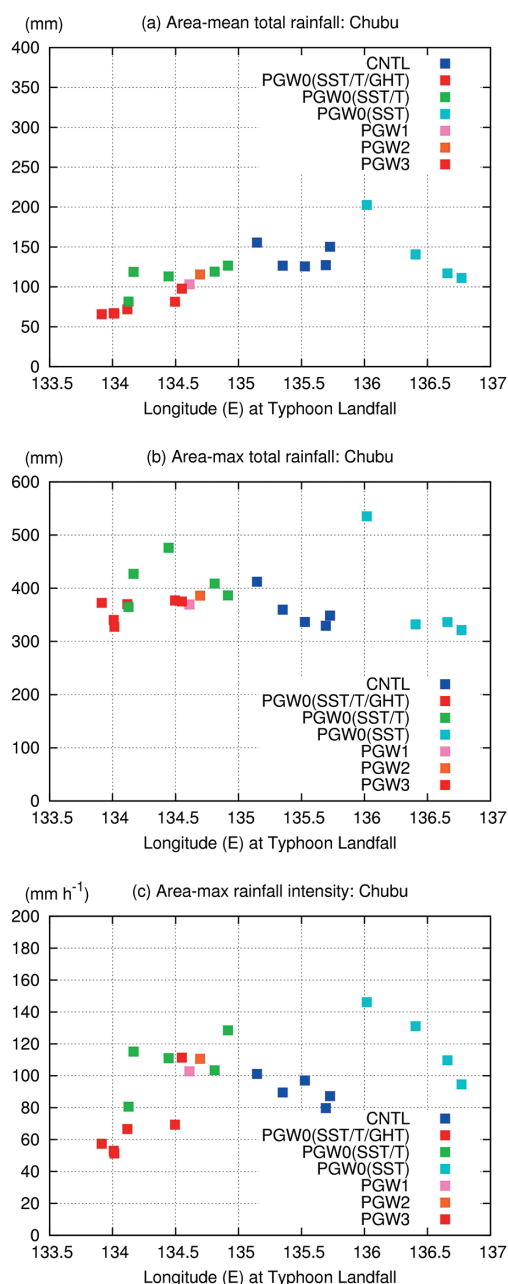
Figure 5. (a) Area-mean total rainfall averaged over the Chubu area, (b) area-maximum total rainfall within the Chubu area, and (c) area-maximum rainfall intensity within the Chubu area

Figure 6. The same as Figure 5, except for the Kinki area

CNTL. There is a PGW case which indicates the maximum total rainfall close to 500 mm, still demonstrating a larger amount than the CNTL cases. The area-maximum rainfall intensity (i.e., hourly rainfall) in the Chubu area also indicates that stronger rain is reproduced in some PGW cases than in the CNTL cases especially when the landfall position in PGW is around 134.5–135.0°E (Figure 5c). In this way, both area-maximum total rainfall and area-maximum hourly rainfall at the worst levels demonstrate larger values in the PGW conditions than in CNTL, despite that there is inevitably dependence to the landfall location.

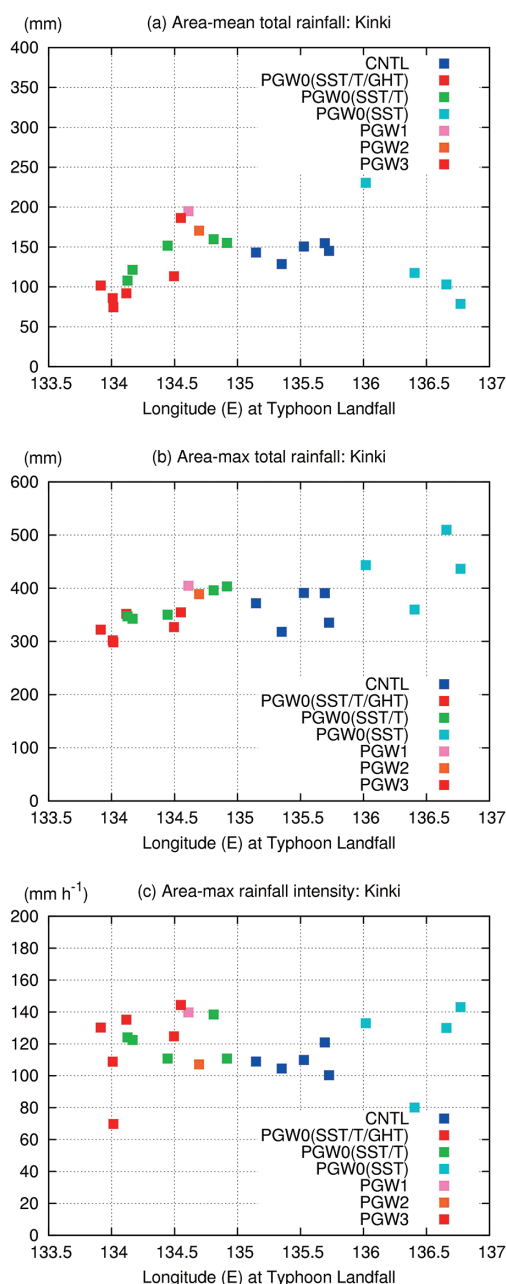The rainfall characteristics are examined for the Kinki

area and are shown in Figure 6. A feature different from the Chubu case is seen for the area-mean total rainfall (Figure 6a). Some cases of the PGW experiments, if the typhoons landed around the 134.5–135.0°E locations, indicate larger amounts of the mean total rainfall than those in CNTL. The area-maximum total rainfall (Figure 6b) and the area-maximum hourly rainfall (Figure 6c) at the worst levels also show larger amounts in cases of the PGW experiments, especially for the cases with the landfall position being in the 134.5–135.0°E range, than in the CNTL cases. Although the effects of the difference in the typhoon tracks between CNTL and PGW are also included in the rainfall characteristics shown in Figures 5 and 6, larger amounts of mean total rainfall, maximum total rainfall, and maximum hourly rainfall in the PGW conditions than in CNTL are more clearly found in

the Kinki area than in the Chubu area.

The effects of the typhoon track on regional-scale rainfall characteristics can be estimated by generating a large ensemble of simulated typhoons having a variety of tracks with the use of the potential vorticity (PV) inversion and typhoon-vortex relocation technique (Ishikawa *et al.*, 2013; Oku *et al.*, 2014). By artificially generating a number of typhoons with their tracks varied, the dependence of heavy rain and strong wind to the track of typhoons can be examined, and the worst typhoon that produces the largest rainfall amount or the strongest wind can be searched. The previous analysis on the effects of the track changes on the rainfall and river discharge over the Yodo River basin demonstrated that the worst typhoon that produced the largest amount of rainfall and river discharge moves along the track very similar to the actual track of Typhoon Vera (Miyawaki *et al.*, 2016). Therefore, larger amounts of rainfall produced by Typhoon Vera in the PGW conditions than in CNTL in spite of the difference in typhoon tracks (Figures 5 and 6) suggests that the amount of rainfall in the PGW conditions would be much larger if the simulated typhoons take the same track as those in CNTL and the actual Typhoon Vera (1959).

CONCLUSIONS

This study investigates the influences of global warming on the intensity and rainfall characteristics of Typhoon Vera (1959) by conducting PGW experiments with the use of the 20-km-mesh AGCM outputs. It was found that the intensity of Typhoon Vera will be stronger in warmed climate conditions than in the actual September 1959 condition not only at the time of the typhoon's maximum intensity during its lifetime but also at the time of the landfall. This projected increase in the typhoon intensity is robust, irrespective of the initial times of the simulations, the added variables as the warming increments, and the AGCM future runs with different SST conditions. From sensitivity experiments with the added warming increments being varied, it was found that an extreme case in which only the SST increment is added produces extremely strong typhoons. Although the stability change under global warming affects negatively the typhoon intensity, the intensity of Typhoon Vera in the PGW conditions will increase.

From the examination of rainfall characteristics over the Kiso River and the Yodo River basin, it was found that the maximum accumulated rainfall and the maximum hourly rainfall at any location within the region are more intensified in the PGW conditions than in the CNTL condition, even by taking into account the difference in the typhoon track between CNTL and PGW. This projected change is considered to be a robust signal as an impact of Typhoon Vera under global warming. On the other hand, there is inevitably dependence to the track of typhoons in considering regional-scale rainfall characteristics over specific basins. It is not easy to completely control the typhoon track irrespective of any atmospheric conditions. However, this uncertainty may be overcome by employing the PV inversion and relocation technique of Ishikawa *et al.* (2013) and generating an ensemble of typhoons with various tracks. Combining this technique with the PGW experiments will offer more precise assessments on the impacts of extreme typhoons.

Although we have demonstrated robust signals of the projected changes in the typhoon impacts in warmed climate by conducting the PGW experiments, there are limitations resulting from the use of the climatological-mean warming increments. For example, we have not taken into account the interannual variability of SST. If SST in a specific future year is much higher than the climatological mean, such a higher SST condition would enhance the development of typhoons; in this case worst-class typhoons considered in this study would be much worse. More elaborate methods for the PGW experiments should be explored in future studies.

SUPPLEMENTS

Text S1. Discussion on the use of TC bogus scheme
Figure S1. The spatial distribution of the warming increments for sea and land surface temperature in (a) PGW0, (b) PGW1, (c) PGW2, and (d) PGW3
Figure S2. The same as Figure S1, except for surface air temperature

REFERENCES

Ebita A, Kobayashi S, Ota Y, Moriya M, Kumabe R, Onogi K, Harada Y, Yasui S, Miyaoka K, Takahashi K, Kamahori H, Kobayashi C, Endo H, Soma M, Oikawa Y, Ishimizu T. 2011. The Japanese 55-year Reanalysis "JRA-55": An interim report. *SOLA* **7**: 149–152. DOI: 10.2151/sola.2011-038.

Harada Y, Kamahori H, Kobayashi C, Endo H, Kobayashi S, Ota Y, Onoda H, Onogi K, Miyaoka K, Takahashi K. 2016. The JRA-55 Reanalysis: Representation of atmospheric circulation and climate variability. *Journal of the Meteorological Society of Japan* **94**: 269–302. DOI: 10.2151/jmsj.2016-015.

Hong SY, Lim JOJ. 2006. The WRF Single-Moment 6-Class Microphysics Scheme (WSM6). *Journal of the Korean Meteorological Society* **42**: 129–151.

Hong SY, Noh Y, Dudhia J. 2006. A new vertical diffusion package with an explicit treatment of entrainment processes. *Monthly Weather Review* **134**: 2318–2341. DOI: 10.1175/MWR3199.1.

Ishikawa H, Oku Y, Kim S, Takemi T, Yoshino J. 2013. Estimation of a possible maximum flood event in the Tone River basin, Japan caused by a tropical cyclone. *Hydrological Processes* **27**: 3292–3300. DOI: 10.1002/hyp.9830.

Ito R, Takemi T, Arakawa O. 2016. A possible reduction in the severity of typhoon wind in the northern part of Japan under global warming: A case study. *SOLA* **12**: 100–105. DOI: 10.2151/sola.2016-023.

JMA. 1961. Report of the Ise Bay Typhoon (No. 5915) in September 1959. JMA Technical Report No. 7, JMA, Tokyo (in Japanese with English abstract).

Kain JS. 2004. The Kain-Fritsch convective parameterization: An update. *Journal of Applied Meteorology* **43**: 170–181. DOI:

10.1175/1520-0450(2004)043<0170:TKCPAU>2.0.CO;2.

Kanada S, Takemi T, Kato M, Yamasaki S, Fudeyasu H, Tsuboki K, Arakawa O, Takayabu I. 2016. A multi-model intercomparison of an intense typhoon in future, warmer climates by four 5-km-mesh model. *Journal of Climate* (under review).

Kitoh A, Endo H. 2016. Changes in precipitation extremes projected by a 20-km mesh global atmospheric model. *Weather and Climate Extremes* **11**: 41–52. DOI: 10.1016/j.wace.2015. 09.001.

Kobayashi S, Ota Y, Harada Y, Ebita A, Moriya M, Onoda H, Onogi K, Kamahori H, Kobayashi C, Endo H, Miyaoka K, Takahashi K. 2015. The JRA-55 Reanalysis: General specifications and basic characteristics. *Journal of the Meteorological Society of Japan* **93**: 5–48. DOI: 10.2151/jmsj.2015-001.

Kusunoki S. 2016. Is the global atmospheric model MRI-AGCM3.2 better than the CMIP5 atmospheric models in simulating precipitation over East Asia? *Climate Dynamics*. DOI: 10.1007/ s00382-016-3335-9 (in press).

Miyawaki K, Tachikawa Y, Tanaka T, Ishii D, Ichikawa Y, Yorozu K, Takemi T. 2016. Flood runoff simulations in the Yodo River basin assuming largest-class typhoons. *Journal of Japan Society of Civil Engineers, Series B1 (Hydraulic Engineering)* **72**: I_31–I_36 (in Japanese with English abstract).

Mizuta R, Arakawa O, Ose T, Kusunoki S, Endo H, Kitoh A. 2014. Classification of CMIP5 future climate responses by the tropical sea surface temperature changes. *SOLA* **10**: 167–171. DOI: 10.2151/sola.2014-035.

Mizuta R, Yoshimura H, Murakami H, Matsueda M, Endo H, Ose T, Kamiguchi K, Hosaka M, Sugi M, Yukimoto S, Kusunoki S, Kitoh A. 2012. Climate simulations using MRI-AGCM3.2 with 20-km grid. *Journal of the Meteorological Society of Japan* **90A**: 233–258. DOI: 10.2151/jmsj.2012-A12.

Mori N, Takemi T. 2016. Impact assessment of coastal hazards due to future changes of tropical cyclones in the North Pacific Ocean. *Weather and Climate Extremes* **11**: 53–69. DOI: 10.1016/j.wace.2015.09.002.

Mori N, Kato M, Kim S, Mase H, Shibutani Y, Takemi T, Tsuboki K, Yasuda T. 2014. Local amplification of storm surge by Super Typhoon Haiyan in Leyte Gulf. *Geophysical Research Letters* **41**: 5106–5113. DOI: 10.1002/2014GL060689.

Murakami H, Wang Y, Yoshimura H, Mizuta R, Sugi M, Shindo E, Adachi Y, Yukimoto S, Hosaka M, Kusunoki S, Ose T, Kitoh A. 2012. Future changes in tropical cyclone activity projected by the new high-resolution MRI-AGCM. *Journal of Climate* **25**: 3237–3260. DOI: 10.1175/JCLI-D-11-00415.1.

National Astronomical Observatory of Japan. 2015. Chronological Scientific Tables. Maruzen Publishing Co., Ltd., Tokyo, Japan; 1098.

Oku Y, Yoshino J, Takemi T, Ishikawa H. 2014. Assessment of heavy rainfall-induced disaster potential based on an ensem-ble simulation of Typhoon Talas (2011) with controlled track and intensity. *Natural Hazards and Earth System Sciences* **14**: 2699–2709. DOI: 10.5194/nhess-14-2699-2014.

Oku Y, Takemi T, Ishikawa H, Kanada S, Nakano M. 2010. Representation of extreme weather during a typhoon landfall in regional meteorological simulations: A model intercomparison study for Typhoon Songda (2004). *Hydrological Research Letters* **4**: 1–5. DOI: 10.3178/hrl.4.1.

Santer BD, Thorne PW, Haimberger L, Taylor KE, Wigley TML, Lanzante JR, Solomon S, Free M, Gleckler PJ, Jones PD, Karl TR, Klein SA, Mears C, Nychka D, Schmidt GA, Sherwood SC, Wentz FJ. 2008. Consistency of modelled and observed temperature trends in the tropical troposphere. *International Journal of Climatology* **28**: 1703–1722. DOI: 10.1002/joc.1756.

Sato T, Kimura F, Kitoh A. 2007. Projection of global warming onto regional precipitation over Mongolia using a regional climate model. *Journal of Hydrology* **333**: 144–154. DOI: 10.1016/j.jhydrol.2006.07.023.

Skamarock WC, Klemp JB, Dudhia J, Gill DO, Barker DM, Duda MG, Huang XY, Wang W, Powers JG. 2008. A description of the Advanced Research WRF version 3. *NCAR Technical Note*, NCAR/TN-47 + STR: 113.

Takayabu I, Hibino K, Sasaki H, Shiogama H, Mori N, Shibutani Y, Takemi T. 2015. Climate change effects on the worst-case storm surge: A case study of Typhoon Haiyan. *Environmental Research Letters* **10**: 064011. DOI: 10.1088/1748-9326/10/6/ 064011.

Takemi T, Nomura S, Oku Y, Ishikawa H. 2012. A regional-scale evaluation of changes in environmental stability for summertime afternoon precipitation under global warming from super-high-resolution GCM simulations: A study for the case in the Kanto Plain. *Journal of the Meteorological Society of Japan* **90A**: 189–212. DOI: 10.2151/jmsj.2012-A10.

Takemi T, Ito R, Arakawa O. 2016a. Effects of global warming on the impacts of Typhoon Mireille (1991) in the Kyushu and Tohoku regions. *Hydrological Research Letters* **10**: 81–87. DOI: 10.3178/hrl.10.81.

Takemi T, Okada Y, Ito R, Ishikawa H, Nakakita E. 2016b. Assessing the impacts of global warming on meteorological hazards and risks in Japan: Philosophy and achievements of the SOUSEI program. *Hydrological Research Letters* (accepted).

Thorne PW, Lanzante JR, Peterson TC, Seidel DJ, Shine KP. 2010. Tropospheric temperature trends: history of an ongoing controversy. *WIREs Climate Change* **2**: 66–88. DOI: 10.1002/ wcc.80.

Wang W, Bruyère C, Duda M, Dudhia J, Gill D, Lin HC, Michalakes J, Rizvi S, Zhang X. 2010. ARW Version 3 Modeling System User's Guide. Mesoscale and Microscale Meteorology Division, National Center for Atmospheric Research; 312.